The benzene radical anion: A computationally demanding prototype for aromatic anions

Article *in* The Journal of Chemical Physics · May 2015

DOI: 10.1063/1.4921261 · Source: PubMed

3 authors, including:

Alexandre Patrick Bazante
University of Florida
7 PUBLICATIONS **50** CITATIONS
SEE PROFILE

Rodney J. Bartlett
University of Florida
709 PUBLICATIONS **53,390** CITATIONS
SEE PROFILE

The benzene radical anion: A computationally demanding prototype for aromatic anions

Alexandre P. Bazante, E. R. Davidson, and Rodney J. Bartlett

Citation: The Journal of Chemical Physics **142**, 204304 (2015); doi: 10.1063/1.4921261
View online: http://dx.doi.org/10.1063/1.4921261
View Table of Contents: http://scitation.aip.org/content/aip/journal/jcp/142/20?ver=pdfcov
Published by the AIP Publishing

The benzene radical anion: A computationally demanding prototype for aromatic anions

Alexandre P. Bazante,[1,a)] E. R. Davidson,[2] and Rodney J. Bartlett[1]
[1]*Quantum Theory Project, University of Florida, Gainesville, Florida 32611, USA*
[2]*Department of Chemistry, University of Washington, Seattle, Washington 98195, USA*

(Received 6 April 2015; accepted 6 May 2015; published online 26 May 2015)

The benzene radical anion is studied with *ab initio* coupled-cluster theory in large basis sets. Unlike the usual assumption, we find that, at the level of theory investigated, the minimum energy geometry is non-planar with tetrahedral distortion at two opposite carbon atoms. The anion is well known for its instability to auto-ionization which poses computational challenges to determine its properties. Despite the importance of the benzene radical anion, the considerable attention it has received in the literature so far has failed to address the details of its structure and shape-resonance character at a high level of theory. Here, we examine the dynamic Jahn-Teller effect and its impact on the anion potential energy surface. We find that a minimum energy geometry of C_2 symmetry is located below one D_{2h} stationary point on a C_{2h} pseudo-rotation surface. The applicability of standard wave function methods to an unbound anion is assessed with the stabilization method. The isotropic hyperfine splitting constants (A_{iso}) are computed and compared to data obtained from experimental electron spin resonance experiments. Satisfactory agreement with experiment is obtained with coupled-cluster theory and large basis sets such as cc-pCVQZ. © *2015 AIP Publishing LLC.* [http://dx.doi.org/10.1063/1.4921261]

INTRODUCTION

The benzene radical anion is of interest in multiple areas of research. It has a ubiquitous presence as an intermediate in several industrial processes. It is also a prototype for anions of the widely studied polyaromatic hydrocarbons (PAHs). Because the benzene radical anion is a transient species that only exists as a resonance state in the gas phase, there are little experimental data.

The novel experiment from Tuttle and Weissman in 1958[1] subjected the benzene molecule to an alkali metal mirror and subsequently measured the experimental electron spin resonance (ESR) spectra of the anion produced to obtain a value for the proton isotropic hyper-fine coupling constant, a_H, of 3.75 G with unknown sign. They recognized that there could be a Jahn-Teller effect making the protons inequivalent but they saw only one value indicating that the protons were equivalent on the time scale of the experiment. Later, an experiment of Bolton and Carrington in 1961[2] using a sodium film provided the same value for a_H. Bolton[3] also measured the ^{13}C hyperfine for benzene anion containing one ^{13}C center and obtained a value of $|a_C|$ of 2.8 G. Lawler and Fraenkel[4] measured the deuterium and proton hyperfine with various numbers of protons replaced by deuteriums. One interesting result from this was that the vibrationally averaged spin density at hydrogen in C_6D_6 is only 94.5% of the spin density in C_6H_6. They also verified that the spin density was temperature dependent (as reported previously by Fessenden[5]) indicating that higher vibrational levels contribute to the thermal average in the 150 K–250 K temperature range.

The hyperfine interaction measures the spin density at the nucleus. Since in naive MO theory the proton and carbon atoms lie in the nodal plane of the π orbital containing the unpaired electron, the hyperfine interaction might be expected to be zero. McConnell[6–9] showed how exchange interactions with the σ bond electrons could lead to a non-zero *negative* value at the proton which was proportional to the population of unpaired π electrons on the neighboring carbon. The empirical proportionality factor, commonly called Q, varies somewhat between molecules. The temperature dependence of a_H is also commonly absorbed into a temperature dependent Q. In spite of these small variations, this relation is widely used to obtain an experimental π spin population from an experimental proton hyperfine. Bolton rationalized his ^{13}C result using a similar relation by Karplus and Fraenkel.[9]

Pople and Beveridge[10] viewed a_N for planar aromatic molecules as arising from the innate magnetic moment for an atom multiplied by the unpaired spin population of the s valence orbital on that atom obtained from a unrestricted Hartree-Fock (UHF) INDO calculation. The innate moment was obtained by a least squares fit to experimental data for a large list of molecules. This approach yielded the value of −3.6 G and +4.0 G for H and ^{13}C a_N in the benzene anion.[10]

Yet, despite the fact that the importance of the benzene anion to the ESR field rivals that of the methyl radical, there are no *ab initio* studies of its A_{iso}. Part of the reason is that the anion offers a major challenge to today's "predictive" *ab initio* correlated theory. To provide the quality of result demanded, the theory has to account for its transient nature as a shape resonance, i.e., of single-particle character, in the gas phase.

a)Author to whom correspondence should be addressed. Electronic mail: abazante@chem.ufl.edu

This resonance has been measured quite precisely by Sanche and Schulz[11] using electron transmission spectroscopy as lying 1.1 eV above the energy of neutral benzene. Curiously, the benzene anion seems to be stable in the condensed phase where the ESR measurements are made and also in a high pressure N_2 atmosphere (Christophorou and Goans[12]). Empirical models to explain the ESR have ignored any effect from the solvent on the hyperfine value or the molecular structure.

In addition, such a high-symmetry anion has to undergo Jahn-Teller distortion and pseudo-rotation to correctly account for its structure. Empirical models which attempt to account for the hyperfine interaction have concluded that the anion is a dynamic Jahn-Teller case (McConnell and McLachlan,[13] Hobey and McLachlan,[14] and Purins and Karplus[15]). The unpaired electron is assumed to go into the lowest empty e_{2u} orbital of benzene. This gives an E_{2u} state which splits into B_{1u} and A_u upon distortion along the e_{2g} active Jahn-Teller modes giving a potential surface with the familiar "Mexican hat" shape. The stationary points on this surface have D_{2h} symmetry. Empirical estimates place the energy lowering from D_{6h} to be around 400 cm^{-1}. The A_u state is higher than B_{1u} by less than 17 cm^{-1}. These barriers are lower than the zero point energies for pseudo-rotation or vibration through the D_{6h} apex of the cone so this is an example of dynamic Jahn-Teller coupling. In the first *ab initio* calculation reported, Hinde *et al.*[16] obtained an energy lowering from D_{6h} of 1900 cm^{-1} and an energy spitting between A_u and B_{1u} of 28 cm^{-1} using CI with a Slater-type orbitals (STO)-3G basis set. They also noted that there was a monotonic downhill path from A_u to B_{1u}. The only other *ab initio* calculation reported to date was by Beregovaya *et al.*[17] who used restricted open-shell Hartree-Fock (ROHF) - second order many body perturbation theory (MBPT(2)) and a 6-31+G* basis set. They obtained an energy splitting of about 125 cm^{-1} between the A_u and B_{1u} doublet states. They did not discuss the energy lowering accompanied by the symmetry reduction from D_{6h}. Similarly, Tokunaga *et al.*[18] extensively studied vibronic coupling in both benzene cation and anion at the benzene neutral geometry and showed how it gives rise to Jahn-Teller distortions; they also show that the magnitude of the coupling originates from the densities in the HOMOs and lowest unoccupied molecular orbitals (LUMOs).

For many years, considerable effort has been devoted to the theoretical determination of isotropic hyper-fine coupling constants (A_{iso})[19–27] for open-shell systems to complement ESR spectroscopy.[28–30] The latter offers perhaps the best probe for the detection of free radicals, especially those of transient nature. As a direct measure of the net unpaired spin density at the nucleus of radicals, the calculation of the spin density provides A_{iso}; however, A_{iso} places demands upon the quality of the wave function produced by quantum chemistry rather than just its associated energy. As a consequence, the calculation of A_{iso} values, which in the normal approximation depend upon the evaluation of a delta function on top of a nucleus, provides a sensitive test of the accuracy of *ab initio* electronic structure theory. This pertains to both the basis set, which has the unenviable task of having to correctly describe a delta function, and the electron correlation which has to be able to accurately account for the differences in the spin density that arises from small differences among all the alpha and beta electrons in the molecule.

Initial CI work[19–24] demonstrated that only with excellent basis sets and large amounts of electron correlation was it possible to obtain fairly accurate results for A_{iso} for atoms. However, the CI methods still suffered from several weaknesses in the treatment of electron correlation due to their lack of size-extensivity which, among other things, would facilitate systematic convergence to the right answer. Many-body methods like coupled-cluster theory[31–33] alleviate many of the prior limitations on the treatment of electron correlation and naturally provide a sequence of improving approximations from coupled cluster singles and doubles (CCSD) (to coupled cluster single and double triple (CCSD(T))) to CCSDT, etc. When these methods are used with a similarly converging sequence of basis sets, preferably extrapolated to the basis set limit,[34,35] predictive results can be obtained.[27] The benzene anion, as a prototype for aromatic anions, warrants this attention.

In the following, the shape resonance is first addressed followed by the Jahn-Teller distortion. After using these to establish the suitability of treating the isotropic coupling constants in a square integrable, L^2 basis, and to determine the relevant distorted geometry, the coupling constants are evaluated using the response density matrix of coupled-cluster theory.[32,33] These matrices are a generalization of the conventional density matrices used in CI, derived from energy derivative theory either with orbital relaxation (relaxed density matrix) or without orbital relaxation (response density matrix). As such, response theory applies to methods like CCSD(T)[33] whose energy is not an expectation value with the associated wave function. The use of coupled cluster density matrices and the generalized expectation value provided has shown exceptional accuracy for a wealth of properties including A_{iso}.[25–27]

EXISTENCE OF BENZENE ANION

High accuracy *ab initio* coupled cluster methods are ordinarily performed in a square-integrable basis set applicable to bound states. Using such methods outside of these parameters may unknowingly produce unphysical results. Therefore, the reported instability of the benzene radical anion must be investigated to determine the validity of subsequent property calculations.

Geometries and frequencies are computed for the benzene neutral using CCSD(T) in the cc-pVTZ basis set. Results are in very good agreement with experimental data and are shown in the supplementary material.[60] As expected from symmetry considerations in MO theory, the LUMOs in neutral benzene are a degenerate pair of e_{2u} symmetry in the D_{6h} point group. Of importance for the section on "Jahn-Teller distortions and pseudo-rotation" are the two e_{2g} low-frequency normal modes. There are two other e_{2g} modes at 1585 cm^{-1} and 3047 cm^{-1} of the correct symmetry to participate in first-order Jahn-Teller distortion. The lowest frequency is the e_{2u} mode which has no first-order effect but has a small force constant which could easily change sign in the anion. This mode represents out of plane motion of the carbon and hydrogen atoms.

TABLE I. Vertical electron affinities for benzene.

Electron affinities (eV)	EA state	cc-pVDZ	cc-pVTZ	cc-pVQZ
Vertical EAs	$B_{1u} \equiv A_u$ (E_{2u})	−2.47	−1.98	−1.79

The vertical electron affinity (EA) for the benzene radical anion may be regarded qualitatively as the energy change upon adding an electron to one of the e_{2u} orbitals. Approximate methods which compute EAs generally neglect both orbital relaxation and correlation to some extent. The errors of these two effects tend to add together, whereas they usually cancel in the case of ionization potentials (IPs). Obtaining accurate results for electron affinities requires, then, the inclusion of both electron correlation and orbital relaxation effects. While relaxation and correlation can be included by optimizing the geometry of the anion with high level coupled cluster and subtracting the energy of neutral benzene from the anion's, correlation effects are computed directly using the electron-attached equation of motion coupled cluster singles and doubles (EA-EOM-CCSD[36]) on neutral benzene. We use the benzene geometry obtained with CCSD(T)/cc-pVQZ and compute the EA-EOM-CCSD[37] eigenvalues in successively larger Dunning type basis sets.

From Table I, we observe that even in large basis sets the benzene radical anion is clearly unbound. Note that for simplicity, the basis sets used here do not contain diffuse functions. The question then arises as to whether it is metastable. The extra electron in the radical anion is located in an orbital of symmetry b_{1u} and a_u, the two components of e_{2u} in the D_{2h} symmetry group. Orbitals with these symmetries are not occupied in neutral benzene which is a good indication that the temporary benzene anion may be characterized as a shape resonance and therefore metastable. The metastability of the benzene anion, and thus the applicability of standard wave function L^2 methods to this problem, is tested using the stabilization method.[38–51] As is commonly done to implement the stabilization method, the lowest roots of an eigenvalue problem for a specific state are tracked by smoothly varying the exponent of diffuse functions on each atom. Resonance parameters can then be extracted by analytically continuing the obtained energies into the complex plane. More details on the stabilization method and the analytic continuation procedure can be found in the supplementary material.[60]

TABLE II. Complex resonance energy of the $^2E_{2u}$ electron attached state of benzene at neutral equilibrium geometry. The numbers in parentheses give the uncertainties in the last decimal obtained from the analytic continuation. The results are almost identical to the ones reported in Ref. 40 as expected.

	E_R (eV)	$\Gamma/2$ (eV)
Analytic continuation	1.594(4)	0.057(4)
Experiment[52]	1.12	~0.06

In this work, we investigate each benzene radical anion states using EA-EOM-CCSD in modified aug-cc-pVTZ basis where one extra diffuse *p* function of exponent 0.04 on each carbon atom is used. The exponent of said function is then scaled by α from 0.1 to 2.0 to construct the stabilization graphs. Test calculations show that additional diffuse *p* functions on the hydrogen atoms have no effect on the resonance parameters.

Figure 1 shows the stabilization graph for the benzene anion doublet state of interest, i.e., $^2E_{2u}$. Note that the first two roots undergo a pronounced avoided crossing around $\alpha = 0.4$, which is indicative of a resonance state. Table II shows the averaged resonance parameters determined by the stabilization method. This shows that the doubly degenerate doublet state under consideration ($^2E_{2u}$) is the lowest energy temporary anion and indeed describes a shape resonance, which has bound-state-like character. As such, that state is appropriately treated by standard CC methods in basis sets as large as aug-cc-pVTZ. Using larger and larger basis sets will eventually break down the ability of wavefunction methods to correctly describe the unbound radical anion as the very diffuse basis functions probe space in which the state of interest is continuum-like.

We also notice that in augmented basis sets, the $^2E_{2u}$ state is not the ground state. This is because application of the variational principle to temporary anions leads to optimum wave functions which describe the neutral species plus a free electron, given flexible enough basis sets. While these bases are important to accurately describe anion properties, one has to be careful to compute those properties for excited states to properly characterize the resonance state rather than a discretized free electron state coupled to the states of the neutral molecule.

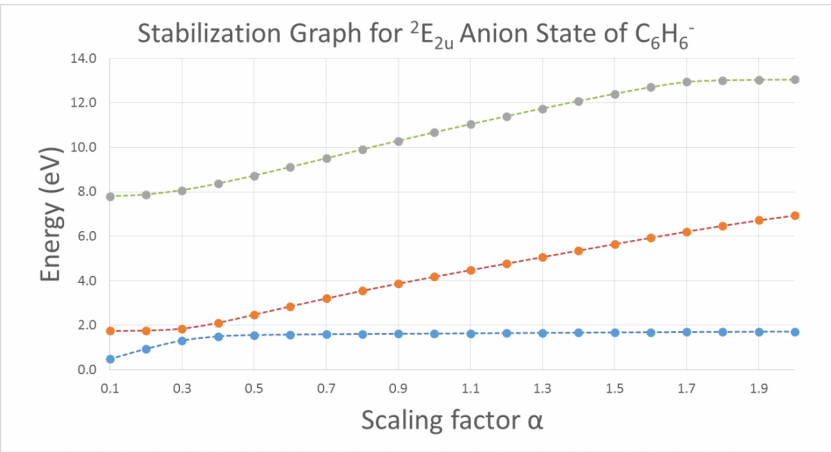

FIG. 1. Stabilization graph of the benzene $^2E_{2u}$ electron attached state with EA-EOM-CCSD. The three data sets correspond to the 1st, 2nd, and 3rd roots of the EA eigenvalue problem in a modified aug-cc-PVTZ basis set.

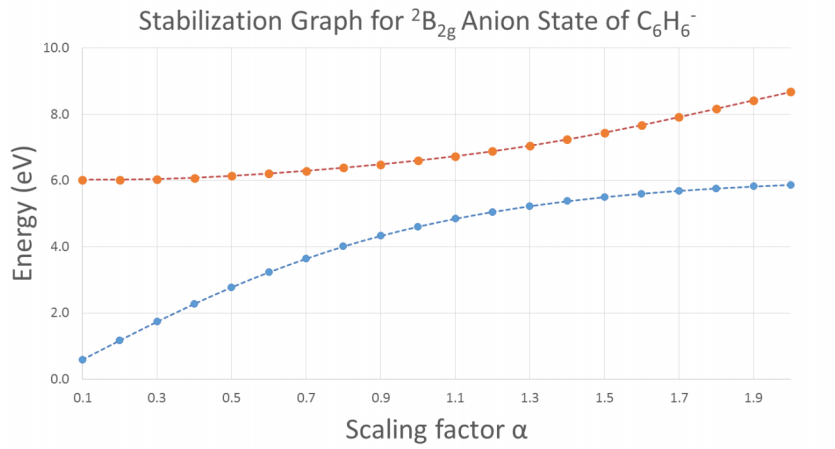

FIG. 2. Stabilization graph of the benzene $^2B_{2g}$ electron attached state with EA-EOM-CCSD. The two data sets correspond to the 1st and 2nd roots of the EA eigenvalue problem in a modified aug-cc-PVTZ basis set.

Additionally, all other relevant states ($^2A_{1g}$, $^2E_{1u}$, $^2E_{2g}$, $^2B_{1u}$, $^2A_{2u}$, $^2E_{1g}$, $^2B_{2u}$, and $^2B_{2g}$) are similarly investigated. Some additional temporary anion states are found that are consistent with the literature, like the $^2B_{2g}$ state. Analytic continuation yields a resonance position of 5.93(2) eV above the neutral with an imaginary part of 0.701(3) eV for the $^2B_{2g}$ temporary anion state, as is shown in Figure 2; the vertical electron affinity is −4.20 eV at the EA-EOM-CCSD/aug-cc-pVTZ level. A resonance in the vicinity has been seen experimentally,[53] with the vertical electron affinity of the corresponding state measured at −4.82 eV.

Jahn-Teller distortion and pseudo-rotation

As mentioned earlier, the LUMOs in neutral benzene are a degenerate pair. From this, it appears that the attachment of an extra electron yields two possible different degenerate states. The Jahn-Teller theorem[54,55] states that any nonlinear molecule in a degenerate electronic state is subject to an instability due to the coupling between electronic and nuclear motions; a distortion along non-totally symmetric vibrational coordinates removes the degeneracy and lowers the energy. Reduction of the spatial symmetry from D_{6h} to the next highest symmetry point group, D_{2h}, allows the two E_{2u} states to split into distinct irreducible representations, A_u and B_{1u}. These two states then relax to two distinct geometries of D_{2h} symmetry.

The symmetry point groups are labeled according to the right-handed coordinate system in which the z axis is perpendicular to the main molecular plane, and the x axis is parallel to the C_1-C_4 axis, as depicted in Figure 3. Unless otherwise specified, subsequent graphic representations of benzene will assume C_1 is placed at the top.

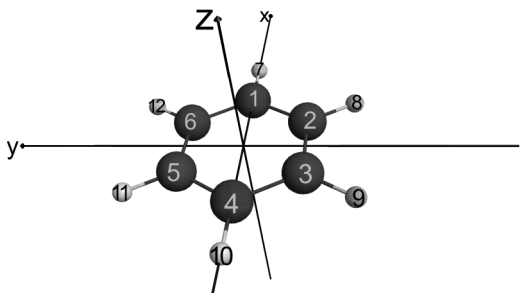

FIG. 3. Right-handed coordinate system used for all benzene calculations.

Both benzene anion structures of interest are optimized with CCSD(T)/cc-pVD(D,T)Z with D_{2h} symmetry constraints. Frozen core calculations are done with a UHF reference using the ACESII software. We find the geometries shown in Table III. In addition, CCSD geometry optimizations have been performed in cc-pVTZ and cc-pVQZ basis sets. The structures obtained show that CCSD(T) geometries are very similar to CCSD geometries on one hand, and that there is very little change between cc-pVTZ and cc-pVQZ on the other hand. We therefore assume that CCSD(T)/cc-pVQZ optimizations would not significantly improve the quality of the geometries. CCSD results are included in the supplementary material.[60] Table III also shows that the relative energy of ^2A_u and $^2B_{1u}$ is reversed by electron correlation relative to the UHF SCF energies.

Optimized bond lengths at UHF-CCSD(T)/cc-pVXZ level (in Å) and relative conformer energies (in kcal/mol).

The optimized anion structures are used to calculate adiabatic electron affinities (AEAs) in a few different ways. First, we simply compute the energy difference between neutral and anion ground states with CCSD(T). AEAs can also be computed using EA-EOM-CCSD by subtracting the neutral ground state energy from the electron attached state energies at the optimized radical anion geometries. Results are shown in Table IV.

As expected, the adiabatic electron affinities are less negative than their vertical counterparts. Augmented basis sets are used to adequately describe the radical electron properties. Because both methods are based on an exponential ansatz, they might be expected to perform well compared

TABLE III. Benzene radical anion CCSD(T) ground state structures.

	$[C_6H_6]^-D_{2h}$ structures			
	^2A_u		$^2B_{1u}$	
Basis (cc-pVXZ)	D	T	D	T
ΔE_{CCSD}	0.04	0.04	0.00	0.00
$\Delta E_{CCSD(T)}$	0.05	0.05	0.00	0.00
r_e (C_3–C_4)	1.473	1.461	1.393	1.380
r_e (C_1–C_2)	1.411	1.399	1.452	1.439
r_e (C_1–H)	1.107	1.091	1.099	1.084
r_e (C_2–H)	1.101	1.085	1.105	1.089

TABLE IV. Adiabatic electron affinities for benzene.

AEAs (eV)	EA state	aug-cc-pVDZ	aug-cc-pVTZ	aug-cc-pVQZ
$\Delta E_{CCSD(T)}$	$D_{2h}\ ^2B_{1u}$	−1.44	−1.41	−1.40
EA-EOM	$D_{2h}\ ^2B_{1u}$	−1.50	−1.44	−1.42

to experiments. The $\Delta E_{CCSD(T)}$ gives the best results since they incorporate perturbative triples corrections. We also demonstrate the ability of EA-EOMCC to compute adiabatic electron attachment energies to an accuracy similar than that of $\Delta E_{CCSD(T)}$ due to the innate cancellation built into EA-EOM. The EA-EOM-CCSD values are slightly more negative than the ones obtained with $\Delta E_{CCSD(T)}$ and very close to what is obtained with ΔE_{CCSD}, not reported here. By comparison, the resonance energy reported in Table II is a lot less accurate since geometry relaxation effects are not included, which is known to be of critical importance for radical anions.

The benzene anion D_{2h} geometries obtained can be depicted as structures distorted from a single hypothetical anion geometry of D_{6h} symmetry with the 4 additional degrees of freedom (Δ, δ, α, and β) associated with the four e_{2g} Jahn-Teller active normal modes. Figure 4 defines the meaning of the parameters and Table V gives their values. For fixed positives values of these parameters, the $^2B_{1u}$ state is found by taking the first sign combination in Figure 4. ^2A_u is obtained with the second combination.

It is known that for a system with 3-fold rotational symmetry, like the benzene radical anion in its hypothetical unstable D_{6h} geometry, the Jahn-Teller distortion results in an adiabatic potential energy surface of C_{3v} symmetry which includes 6 stationary points (3 minima and 3 saddle points).[56] The two-dimensional PES is depicted for the benzene anion in Figure 5. Pseudo-rotations are conformational changes resulting in appearance like an overall rotation of the initial molecule but without actual rotation. The lowest energy pathway connecting the minima on the above potential energy surface is an example of such a conformational change.

It is interesting to notice that there is no point of D_{6h} symmetry along the benzene anion pseudo-rotation path. The sum of squares of C–C bond lengths and C–H bond lengths

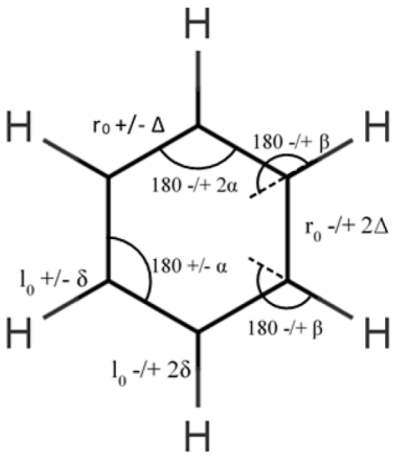

FIG. 4. Jahn-Teller distortions from the D_{6h} to the D_{2h} point group for the benzene radical anion.

TABLE V. Summary of distortions from D_{6h} symmetry for the benzene radical anion optimized structures.

Method	UHF-CCSD(T) optimization			
Bz^- state	^2Au		$^2B_{1u}$	
Basis set	cc-pVDZ	cc-pVTZ	cc-pVDZ	cc-pVTZ
r_0 (Å)	1.432	1.420	1.432	1.420
Δ (Å)	0.021	0.021	0.020	0.020
l_0 (Å)	1.103	1.087	1.103	1.087
δ (Å)	0.002	0.002	0.002	0.002
α (deg)	1.566	1.538	1.628	1.604
β (deg)	−0.327	−0.385	−0.468	−0.531

is the same in both D_{2h} structures, as well as everywhere on the pseudo-rotation path, while this is not the case for the highly symmetric D_{6h} structure; it is characteristic of a constant Jahn-Teller distortion magnitude for all stationary points. This indicates that even at the optimum D_{2h} structures the same linear combination of the four e_{2g} normal modes enters into the distortion.

The interconversion between the adjacent A_u and B_{1u} benzene anion stationary points, i.e., one-sixth of the pseudo-rotational path, occurs via symmetry reduction to the nearest subgroup in which their electronic states have the same irreducible representation. In this case, the C_{2h} point group is encountered along the pseudo-rotational path and occurs through a combination of the a_g and b_{1g} vibrational modes formed from the reduction in symmetry of the e_{2g} mode at D_{6h}.

The distortions ($Q_x = a_g$, $Q_y = b_{1g}$) along this path are determined by the structures of the stationary points and the angle formed with the arbitrarily chosen "top" of the surface.

The distortions satisfy the following equation:

$$Q = Q_x \cos(\theta) + Q_y \sin(\theta), \tag{1}$$

where Q_x and Q_y are the distortions for Θ = 0 and Θ = 90, respectively. The two stationary point distortions may be

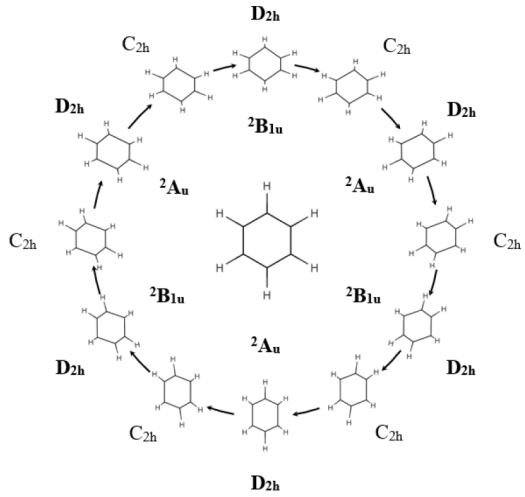

FIG. 5. Two dimensional path of the benzene anion pseudo-rotation for Δ = δ = 0.2 Å, α = 5°, and β = 0°. The 6 stationary points on the D_{2h} surface are represented, as well as some $^2AC_{2h}$ intermediates. Here, C_1 is at the top for all.

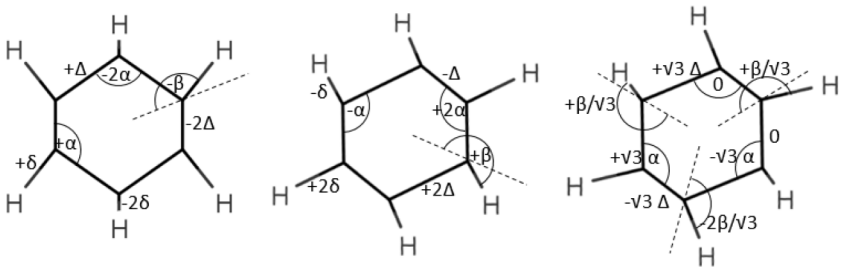

FIG. 6. Structures of pseudo-rotational distortions for two distinct stationary points of the adiabatic potential energy surface and their intermediate. They correspond respectively to distortion coordinates Q at $\Theta = 0°$, 60°, and 90°. The position of C_1 is the same as in Figure 5.

chosen to be $\Theta = 0$ for $^2B_{1u}$ and $\Theta = 60$ for ^2A_u; this equation allows the distortions along the entire path to be determined. Figure 6 depicts Q_x, $Q(\Theta = 60)$, and $Q_y(\Theta = 90)$.

From the optimized CCSD(T) structures in the cc-pVTZ basis, energies at several geometries along the pseudo-rotational path are evaluated using CCSD/cc-pVTZ. This leads to the one dimensional potential energy surface depicted in Figure 7. As one can see, the interconversion between the two doublet states is monotonic, and therefore, there is no transition state along the path. Rather, the A_u state is a transition state of the pseudo-rotation of B_{1u}, documented by the evaluation of harmonic vibrational frequencies for A_u and B_{1u} with CCSD(T)/cc-pVTZ shown in Table VI.

As expected, the one imaginary frequency in the A_u doublet state is found to be a b_{1g} normal mode which breaks the D_{2h} symmetry and represents molecular deformations leading to the B_{1u} minimum on the C_{2h} surface. However, the B_{1u} doublet state possesses imaginary frequencies whose normal modes do not correspond to pseudo-rotation. Distortions of nuclear coordinates along the corresponding normal modes lead to the benzene radical anion global minimum of lower symmetry.

The C_2 ^2A global minimum geometry optimized at the CCSD/cc-pVTZ level is very similar to the D_{2h} $^2B_{1u}$ local minimum. The nuclear repulsion energy differs by 0.019 a.u. and the two sets of all interatomic distances differ by 0.0019 Å on average (0.0072 Å at most). The coordinates for this structure are included in the supplementary material.[60] The b_{1u} orbital localizes the extra charge on the C_1 and C_4 position and reduces the bond order between these carbons and their neighbors. As a consequence, these carbon centers become somewhat pyramidal to give a C_{2v} structure. In addition, there is a slight puckering of the ring at the other carbons leading to the C_2 minimum.

Also represented in Table VI is the point of D_{6h} symmetry, located at the apex of the potential energy surface. This point is a non-differentiable cusp, and as such, first derivatives do not exist. Zero-point energy and vibrational frequencies are only computed as an illustrative tool to demonstrate that the only imaginary frequencies are a degenerate pair of e_{2g} symmetry. There are four degenerate e_{2g} modes in the D_{6h} point group. A linear combination of one Q_x phase from each mode leads to the active Jahn-Teller coordinate with four degrees of freedom going from the D_{6h} geometry to the D_{2h} geometry.

The minimum geometry is used to compute improved adiabatic electron affinities shown in Table VII. These results are obtained using the same method used for Table V.

The AEAs obtained for the C_2 ^2A minimum are very close to the AEAs we report for the D_{2h} $^2B_{1u}$ stationary point in Table V, as expected.

The reversal in relative order of the zero-point energy corrected B_{1u} and A_u structures further shows that this is a dynamic Jahn-Teller effect. In computing the zero-point energy, the local minimum is fit to a parabolic potential, and the harmonic oscillator zero-point is calculated. Table VI shows that the resulting energies lay above the barriers at the transition state. That is, for example, in Figure 7, the harmonic estimate of the zero point energy at the B_{1u} minimum is higher than the A_u barrier. Clearly, the use of a quadratic fit to this potential to estimate the zero point energy produces meaningless numbers. It is also clear that the true zero point is above the barrier and the molecule is almost freely pseudo-rotating.

Furthermore, the pseudo-rotation PES can be computed similarly for different values of the distortion parameters (Δ,

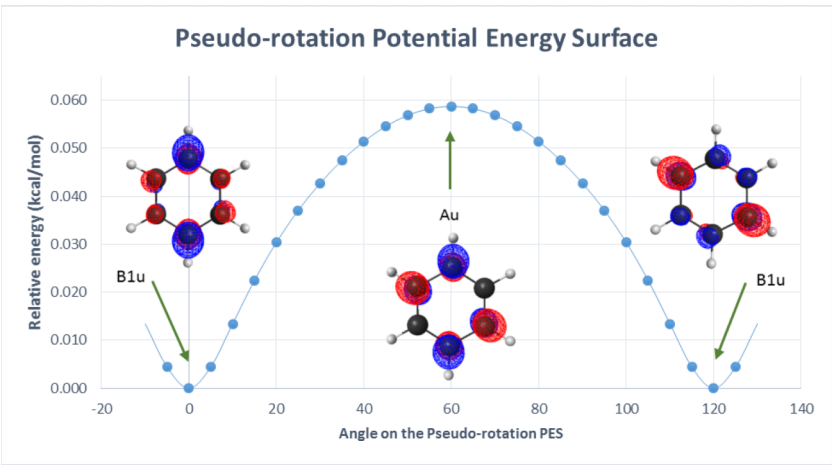

FIG. 7. One dimensional cut through the potential energy surface of the benzene anion along the pseudo-rotation path. Also depicted are the isosurfaces of the HF HOMO, along with the Hückel orbital coefficients for each carbon atoms.

TABLE VI. Stationary points on the $C_6H_6^-$ PES as computed with CCSD(T)/cc-pVTZ. Relative energies are given in kcal/mol.

State	E_{rel}	(ZPE) E_{rel}[a]	N[b]	ν_{imag} (cm^{-1})	Active modes
D_{6h} ($^2E_{2u}$)[c]	2.77	N/A[d]	2[d]	N/A[d]	e_{2g}[d]
D_{2h} ($^2B_{1u}$)	0.07	−0.66	2	266 *i* 204 *i*	b_{1u} b_{2g}
D_{2h} (^2A_u)	0.12	−1.31	1	155 *i*	b_{1g}
C_2 (^2A)[e]	0.00	0.00	0		

[a]Zero-point energy corrected relative energy.
[b]Number of imaginary vibrational frequencies.
[c]Non-stationary point, non-differentiable cusp.
[d]Artifactual.
[e]Global minimum.

δ, α, and β) to create the two-dimensional PES of the pseudo-rotation coupled with the Jahn-Teller distortion. Figure 8 depicts the "Mexican hat" shape of said two-dimensional potential surface obtained when all parameters are varied in concert. In addition, use of a restricted open shell Hartree-Fock reference for the benzene anion geometry optimizations did not have any effect on the final geometries and relative energies. While it is sometimes acknowledged in the literature that UHF theory can lead to erroneous results for Jahn-Teller distorted radicals because of spin contamination issues, here the well-known capacity of infinite order methods such as coupled cluster to recover from a problematic starting point is illustrated. In fact, the spin multiplicity $2S + 1 = (1 + 4\langle S^2\rangle)^{1/2}$ was monitored through every coupled cluster calculation and never deviated from 2 by more than 0.002.

Isotropic hyperfine splitting constant of benzene anion

The isotropic hyperfine splitting constants are given by the Fermi contact splitting term

$$\hat{a}_N = \left(\frac{8\pi}{3}\right)\left(\frac{g_e}{g_0}\right) g_N \beta_N \hat{\rho}(r_N), \tag{2}$$

where $\hat{\rho}(r_N)$ is the spin density operator; $\left(\frac{g_e}{g_0}\right)$ is the ratio of the g values of the free electron and the radical considered and will be taken as unity for the rest of this work. g_N and

TABLE VII. Adiabatic electron affinities for benzene at the minimum geometry.

AEAs (eV)	EA state	aug-cc-pVDZ	aug-cc-pVTZ	aug-cc-pVQZ
$\Delta E_{CCSD(T)}$	C_2 ^2A	−1.66	−1.40	−1.34
EA-EOM	C_2 ^2A	−1.51	−1.42	−1.40

β_N are the nuclear gyromagnetic ratio and Bohr magneton at the various nuclei in the molecule, respectively, sometimes referred to with different names and symbols,

$$g_N = \frac{e\hbar}{2m_P} \approx 5.05 \times 10^{-27}\ \text{J/T}, \tag{3}$$

$$\beta_N = \frac{e\hbar}{2m_e} \approx 9.27 \times 10^{-24}\ \text{J/T}. \tag{4}$$

The isotropic hyperfine splitting constant at each nucleus is computed using

$$A_{iso}\,(\text{MHz}) = 800.2375 * \frac{\mu_N}{I} * \langle \text{spin density} \rangle, \tag{5}$$

$$A_{iso}\,(\text{G}) = 2.802\,494 * A_{iso}(\text{MHz}), \tag{6}$$

with the following values for the C and H atoms:

$$\mu_N\,(^{13}\text{C}) = 0.7024, \tag{7}$$

$$\mu_N\,(^{1}\text{H}) = 2.792\,79. \tag{8}$$

$I = 1/2$ for both nuclei.

To obtain the isotropic hyperfine splitting constants for all distinct atoms in the benzene radical anion using response CCSD(T) theory, as one would expect, core functions are necessary for an accurate computation of spin densities. Using the delta function operator, the splitting constants are obtained in a mixed basis: aug-cc-pCVQZ on the hydrogen atoms and cc-pCVQZ on the carbon atoms. In the benzene radical anion of D_{2h} symmetry, there is one set of 4 and another set of 2 equivalent carbon atoms; and the same for hydrogen atoms. Thus, one obtains 2 different spin density values for hydrogen and carbon. The C_{2h} pseudo-rotation barrier is small, which indicates that each stationary point interconverts rapidly. Therefore, the relevant spin density for

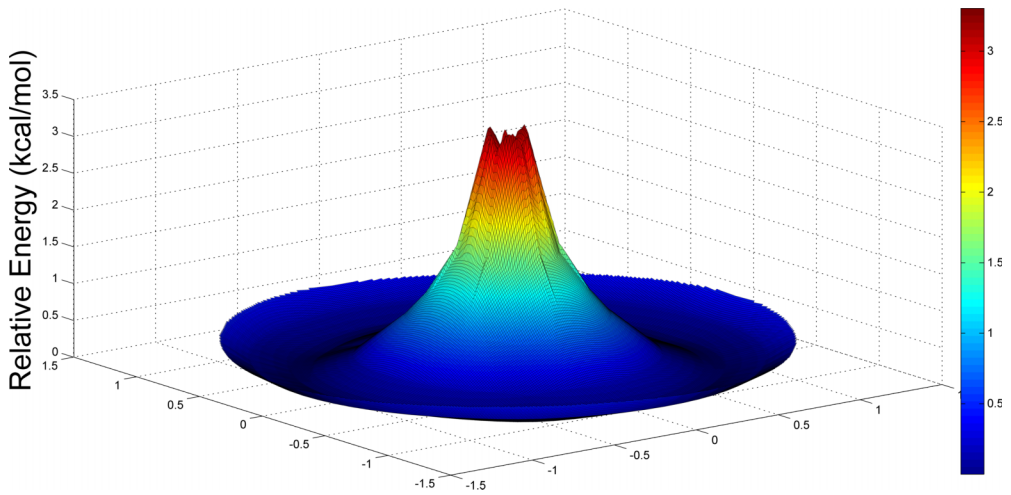

FIG. 8. Three dimensional representation of the two dimensional potential energy surface of benzene anion Jahn-Teller distortion.

TABLE VIII. Calculated benzene anion isotropic hyperfine splitting constants with UHF CCSD(T).

State	E_{rel} (kcal/mol)	Carbon HFS (G)	Hydrogen HFS (G)
C_2 (^{2}A)	−0.07	1.68	−3.70
D_{2h} ($^2B_{1u}$)	0.00	1.39	−4.96
D_{2h} (^2A_u)	0.05	1.31	−4.99

a given atom in the D_{2h} $^2B_{1u}$ state, for example, is the average for that fixed atom over the three equivalent $^2B_{1u}$ structures. The same principle is applied for the C_2 minimum; there are 12 equivalent minima under C2 symmetry and 3 sets of 2 equivalent carbon (equivalently hydrogen) atoms in each of them. Table VIII reports the average for each atom in a given state of interest (D_{2h} $^2B_{1u}$, D_{2h} ^2A_u, and C_2 ^{2}A).

Table VIII shows the computed A_{iso} for the three stationary points of interest. Both D_{2h} points have a similar average for both carbon and hydrogen atoms. The minimum energy doublet geometry, however, has hyperfine splitting constants which differ from its D_{2h} $^2B_{1u}$ form since the atoms are no longer sitting on the nodal plane. The minimum energy geometry gives the best results compared to experiment.

This computed hydrogen isotropic hyperfine coupling constant is very close to the experimental value of −3.75 G. For the carbon A_{iso}, the experimental value is 2.8 ± 0.1 G. Prior work on many radicals[27] have shown that typical values obtained by CCSD(T) methods in TZ2P bases are within ∼10% of experiment for C, while better bases are required for H to provide a 10% error.[57] Here, however, the small value for C causes a larger fractional error.

Another computation uses a ROHF reference instead of the UHF one. As is well known, for a π radical, a ROHF calculation that preserves symmetry has to give a zero A_{iso}. So unlike the UHF based calculation, the entire value of A_{iso} has to be introduced by correlation. But CC theory does this well, providing the following values in Table IX. The aforementioned basis sets were used. These values are consistent with the UHF based calculations, although slightly poorer in quality presumably due to the larger amount of work the CC theory has to perform.

The insensitivity of coupled cluster to orbital choice even makes it possible to form a zeroth order wave function for this anion by simply adding an electron to the lowest unoccupied HF orbital of appropriate symmetry of the neutral molecule at the anion geometry to provide a starting determinant of quasi-RHF (QRHF) form.[58] This means that the reference determinant and its orbitals are not variationally optimized for the anion. QRHF references can only be used in CC calculations because the wave functions have built into them the exp(T1) operator that rotates the reference orbitals as needed. Non-variational QRHF references become useful in many contexts.

TABLE IX. Calculated benzene anion isotropic hyperfine splitting constants with ROHF CCSD(T).

State	E_{rel} (kcal/mol)	Carbon HFS (G)	Hydrogen HFS (G)
C_2 (^{2}A)	−0.07	1.39	−3.62
D_{2h} ($^2B_{1u}$)	0.00	1.10	−4.85
D_{2h} (^2A_u)	0.05	1.02	−4.88

The QRHF and EA-EOM results can be found in the supplementary material,[60] along with the "relaxed" density matrix based results as opposed to response density for all mentioned references. They are consistent with UHF and ROHF based results, demonstrating the power of CC theory to recover from a less than ideal reference determinant.

CONCLUSIONS

This work presents a comprehensive study of the benzene radical anion structure. It demonstrates that at the high level of calculation used, the anion has a non-planar character in contrast to its past use as an example for planar aromatic radicals. The numerical results verify the experimental negative electron affinity, not previously mentioned in published *ab initio* calculations. In agreement with past semi-empirical results, this molecule is shown to manifest a dynamic Jahn-Teller effect that causes it to be fluxional with no fixed structure. Finally, we report gas phase proton and ^{13}C hyperfine interactions that are in reasonable agreement with experimental measurements in solution.

As previously reported in the experimental literature, the benzene radical anion is very clearly unbound in the gas phase leading to an observed scattering resonance. Moreover, the doublet state is a shape resonance, i.e., metastable, allowing some careful experiments to make measurements on the anion even in the condensed phase. The calculated vertical electron affinity (−1.72 eV) and resonance position (−1.59 eV) are consistent with the previously reported experimental adiabatic value of −1.1 eV, which we compute to be ∼1.4 eV. The shape resonance character requires special consideration to assess its relative stability and the validity of standard wave function methods developed for bound states. Using the stabilization method, it is established that the doublet state under consideration is the lowest energy resonant state. Additionally, it has the longest computed lifetime, whose calculated value matches with the experimental data, and it is an electron-attached state of single particle character. All of this shows that the benzene radical anion ground state is a shape resonance whose single particle character allows it to be adequately treated by standard *ab initio* methods, like coupled cluster theory, in square integrable basis sets.

We show the importance of the dynamic Jahn-Teller effect to qualitatively understand the benzene anion potential surface. The study of the pseudo-rotation and Jahn-Teller distortions made it possible to find the structure of the energy minimum. The optimal benzene anion ground state geometry is found to be non-planar of C_2 symmetry. This is a new result as all previous studies predicted (or assumed) a planar D_{2h} structure. The energy lowering by reducing the symmetry constraint from D_{2h} to C_2 is estimated to be ∼0.07 kcal/mol at the CCSD(T)/cc-pVTZ level. Such a small energy difference is easily missed without high level *ab initio* methods and large basis sets. A radical of this moderate size allows for methods such as CCSD(T) to be used and to produce plausible energies and properties, even for an unbound resonance. The

pseudo-rotation, and more generally the potential surface for the benzene radical anion, is rather flat around the energy minimum. Therefore, all stationary points on a given pseudo-rotation path are easily accessible through vibrational modes and observed values for properties should be averages of all equivalent stationary points.

Finally, we report the only *ab initio* study of the hyperfine splitting constants values for the benzene radical anion. While the agreement with experiment for the hydrogen atoms is almost perfect, a very accurate computation of the carbon A_{iso} appears to require even a higher level of theory, more specifically much larger basis sets as is indicated by previous studies.[59] Assuming the experimental value is accurate, the absolute error for carbon is similar to that found previously for CCSD(T), but in this case, it is a much larger fraction compared to the rather small a_C.

ACKNOWLEDGMENTS

We acknowledge useful conversations with Professor John Stanton and Professor Michael Falcetta. This work is supported by the U.S. Air Force Office of Scientific Research (Grant No. FA 9550-11-1-0065).

[1]T. R. Tuttle and S. I. Weissman, J. Am. Chem. Soc. **80**, 5342 (1958).
[2]J. R. Bolton and A. Carrington, Mol. Phys. **4**, 497 (1961).
[3]J. R. Bolton, Mol. Phys. **6**, 219 (1963).
[4]R. G. Lawler and G. K. Fraenkel, J. Chem. Phys. **49**, 1126 (1968).
[5]R. W. Fessenden and S. Ogawa, J. Am. Chem. Soc. **86**, 3591 (1964).
[6]H. M. McConnell, J. Chem. Phys. **24**, 764 (1956).
[7]H. M. McConnell and D. B. Chesnut, J. Chem. Phys. **27**, 984 (1957).
[8]A. Gold, J. Am, Chem. Soc. **91**, 4961 (1969).
[9]M. Karplus and G. K. Fraenkel, J. Chem. Phys. **35**, 1312 (1961).
[10]J. A. Pople and D. L. Beveridge, *Approximate Molecular Orbital Theory* (McGraw-Hill, 1970), p. 214.
[11]L. Sanche and G. Schulz, J. Chem. Phys. **58**, 479 (1973).
[12]L. G. Christophorou and R. E. Goans, J. Chem. Phys. **60**, 4244 (1974).
[13]H. M. McConnell and A. D. McLachlan, J. Chem. Phys. **34**, 1 (1961).
[14]W. D. Hobey and A. D. McLachlan, J. Chem. Phys. **33**, 1695 (1960).
[15]D. Purins and M. Karplus, J. Chem. Phys. **62**, 320 (1975).
[16]A. L. Hinde, D. Poppinger, and L. Radom, J. Am. Chem. Soc. **100**, 4681 (1978).
[17]I. V. Beregovaya and L. N. Shchegoleva, Int. J. Quantum Chem. **88**, 481 (2002).
[18]K. Tokunaga, T. Sato, and K. Tanaka, J. Chem. Phys. **124**, 154303 (2006).
[19]S. Y. Chang, E. R. Davidson, and W. Vincow, J. Chem. Phys. **52**, 1740 (1970).
[20]Y. Ellinger, A. Rassat, R. Subra, and G. Berthier, J. Chem. Phys. **62**, 1 (1975).
[21]D. Feller and E. R. Davidson, J. Chem. Phys. **80**, 1006 (1984).
[22]D. Feller and E. R. Davidson, in *Theoretical Models of Chemical Bonding Part 3. Molecular Spectroscopy, Electronic Structure and Intramolecular Interactions*, edited by Z. B. Maksic (Springer-Verlag, Berlin, 1991), pp. 429–455.
[23]C. W. Bauschlicher, S. R. Langhoff, H. Partridge, and D. P. Chong, J. Chem. Phys. **89**, 2985 (1988).
[24]D. Chipman, Phys. Rev. A **39**, 475 (1989).
[25]H. Sekino and R. J. Bartlett, J. Chem. Phys. **82**, 4225 (1985).
[26]S. A. Perera, J. D. Watts, and R. J. Bartlett, J. Chem. Phys. **100**, 1425 (1994).
[27]S. A. Perera, L. M. Salemi, and R. J. Bartlett, J. Chem. Phys. **106**, 4061 (1997).
[28]W. J. Welter, *Magnetic Atoms and Molecules* (Scientific and Academic Editions, New York, 1983).
[29]L. B. Knight, M. B. Wise, E. R. Davidson, and L. E. McMurchie, J. Chem. Phys. **76**, 126 (1982).
[30]L. B. Knight, J. Steadman, P. K. Miller, D. E. Bowman, E. R. Davidson, and D. Feller, J. Chem. Phys. **80**, 4593 (1984).
[31]R. J. Bartlett, Annu. Rev. Phys. Chem. **32**, 359 (1981).
[32]R. J. Bartlett, J. Phys. Chem. **93**, 1697 (1989).
[33]R. J. Bartlett and M. Musiał, Rev. Mod. Phys. **79**, 291 (2007).
[34]J. G. Hill, K. A. Peterson, G. Knizia, and H.-J. Werner, J. Chem. Phys. **131**, 194105 (2009).
[35]T. Helgaker, P. Jorgensen, and J. Olsen, *Molecular Electronic-Structure Theory* (Wiley, Chichester, 2000), p. 938.
[36]J. F. Stanton and R. J. Bartlett, J. Chem. Phys. **98**, 7029 (1993).
[37]M. Nooijen and R. J. Bartlett, J. Chem. Phys. **102**, 3629 (1995).
[38]A. Hazi and H. Taylor, Phys. Rev. A **1**, 1109 (1970).
[39]H. Taylor and A. Hazi, Phys. Rev. A **14**, 2071 (1976).
[40]M. F. Falcetta, L. A. DiFalco, D. S. Ackerman, J. C. Barlow, and K. D. Jordan, J. Phys. Chem. A **118**, 7489 (2014).
[41]J. S.-Y. Chao, M. F. Falcetta, and K. D. Jordan, J. Chem. Phys. **93**, 1125 (1990).
[42]M. F. Falcetta and K. D. Jordan, J. Phys. Chem. **94**, 5666 (1990).
[43]M. F. Falcetta and K. D. Jordan, Chem. Phys. Lett. **300**, 588 (1999).
[44]K. Y. Ho and S. S. Tan, Chin. J. Phys. **35**, 701 (1997).
[45]H.-Y. Cheng, C.-W. Chen, and C.-H. Huang, J. Phys. Chem. A **116**, 3224 (2012).
[46]H.-Y. Cheng, C.-W. Chen, J.-T. Chang, and C.-C. Shih, J. Phys. Chem. A **115**, 84 (2011).
[47]H.-Y. Cheng and C.-W. Chen, J. Phys. Chem. A **115**, 10113 (2011).
[48]H.-Y. Cheng, J.-T. Chang, and C.-C. Shih, J. Phys. Chem. A **114**, 2920 (2010).
[49]H.-Y. Cheng and C.-C. Shih, J. Phys. Chem. A **113**, 1548 (2009).
[50]H.-Y. Cheng, C.-C. Shih, and J.-T. Chang, J. Phys. Chem. A **113**, 9551 (2009).
[51]Y.-H. Wei and H.-Y. Cheng, J. Phys. Chem. A **102**, 3560 (1998).
[52]K. D. Jordan and P. D. Burrow, Chem. Rev. **87**, 557 (1987).
[53]S. Wong and G. Schulz, Phys. Rev. Lett. **35**, 1429 (1975).
[54]H. A. Jahn and E. Teller, Proc. R. Soc. A **161**, 220 (1937).
[55]I. B. Bersuker, *The Jahn–Teller Effect* (Cambridge University Press, 2006).
[56]I. B. Bersuker and V. Z. Polinger, *Vibronic Interactions in Molecules and Crystals* (Springer-Verlag, 1989), p. 422.
[57]S. Fau and R. J. Bartlett, J. Phys. Chem. A **107**, 6648 (2003).
[58]M. Rittby and R. J. Bartlett, J. Phys. Chem. **92**, 3033 (1988).
[59]D. Feller and E. R. Davidson, J. Chem. Phys. **88**, 7580 (1988).
[60]See supplementary material at http://dx.doi.org/10.1063/1.4921261 for (i) coupled cluster results for neutral benzene as well as CCSD results for the benzene radical anion; (ii) Cartesian coordinates for all three optimized benzene anion state, along with details on the stabilization method and the analytic continuation procedure; and (iii) isotropic hyperfine splitting constants calculations for different coupled cluster references and density matrix approaches.